



ELSEVIER

Computer Physics Communications 145 (2002) 371–384

Computer Physics
Communications

www.elsevier.com/locate/cpc

Recognition and analysis of local structure in polycrystalline configurations [☆]

Igor Stankovic ^{a,*}, Martin Kröger ^{a,b}, Siegfried Hess ^a

^a *Institut für Theoretische Physik PN 7-1, Technische Univ. Berlin, D-10623 Berlin, Germany*

^b *Polymerphysik, Department of Materials, ETH Zürich, CH-8092 Zürich, Switzerland*

Received 10 September 2001; received in revised form 20 December 2001

Abstract

A method is described for obtaining information about the local order existing in monoatomic model solids or real materials based on their atomistic configurations. An efficient algorithmic implementation is provided. The shape of the polyhedra formed by 'relevant' neighbors of each atom enter a pattern recognition method to resolve the type of the (usually non-ideal) crystal structure to which atoms surrounded by their relevant neighbors belong: hexagonal close-packed, face-centered cubic or body-centered cubic. Further, this approach allows for the analysis of icosahedral structure which preferably occurs in amorphous solids. Results of a molecular dynamics computer simulation illustrate how this method can be applied to contribute to an understanding of the mechanical and structural properties of solids (i) undergoing a steady shear stress and (ii) upon increasing temperature. © 2002 Elsevier Science B.V. All rights reserved.

PACS: 61.20.-p; 83.50.-v; 61.46.+w; 61.90.+d

Keywords: Local structure; Recognition; Algorithm; Configuration analysis; Non-ideal lattices; Metal

PROGRAM SUMMARY

Title of program: RLSCODE

Catalogue identifier: ADPZ

Program Summary URL: <http://cpc.cs.qub.ac.uk/summaries/ADPZ>

Program obtainable from: CPC Program Library, Queen's University of Belfast, N. Ireland

Licensing provisions: Persons requesting the program must sign the standard CPC-non-profit use license (see license agreement printed in every issue)

Computer for which the program is designed and others on which it has been tested: Alpha-Workstation, Silicon Graphics, Sun, Linux-PC, Windows-PC, MacIntosh

Operating systems or monitors under which the program has been tested: DEC-Unix, Irix, Solaris, Linux, Windows 98

Program language used: Fortran, MathematicaTM

[☆] This program can be downloaded from the CPC Program Library under catalogue identifier: <http://cpc.cs.qub.ac.uk/summaries/ADPZ>

* Corresponding author.

E-mail address: stankovic@itp.physik.tu-berlin.de (I. Stankovic).

Table 1
Summary of source files of the RLSCODE package

Code file name	Lines	Content
<i>structure.f</i>	356	main program
<i>inc.order</i>	2224	contains all subroutines
Configuration file name	Particles #	Content
<i>fckembed.temp=0.00500..0.06440</i>	10976	configurations, melting of fcc
<i>bckembed.temp=0.00500..0.06440</i>	11664	configurations, melting of bcc
<i>output.shearT=0.008</i>	17576	system under shear flow

Memory required to execute with typical data: 10 MBytes

No. of lines in distributed program: 2224

No. of bytes in distributed program, including test data, etc.:
51 555 974

Distribution format: tar gzip file

Number of lines in distributed program and number of fields in distributed test data is summarized in Table 1

Keywords: Structure recognition, algorithm, configuration analysis, metal

Nature of physical problem

The nature of the problem is to provide a quantitative measure for the local order in non-ideal crystalline configurations. This measure

will be necessarily heuristic in nature and not unique. Configurations are specified by collection of particle position in 3D. The program should return the type of local structure (face centered cubic, etc.) for each atom of the system.

Method of solution

The method is based on a suitable definition for 'neighboring atoms'. The corresponding neighbor list, together with information about correlations between neighbors, is used to uniquely recognize a number of representative crystal structures. The criteria for the recognition of different crystal structures is formulated using graphs.

Restrictions on the complexity of the problem

The machine must provide the necessary main memory which increases roughly linearly with the number of particles.

Typical running time

A typical running time is less than 20 s for 10,000 particles on a 600 MHz Pentium processor.

LONG WRITE-UP

1. Introduction

Recent computer simulations of structural phase transitions and plastic flow of model solids [1–4] prove a need for an analysis which offers a detailed picture about local- and nanostructures on a scale from single to several atoms. The method to be outlined provides the amount and spatial distribution of different structures at every time step, recognizes the amorphous regions and yields information about orientation and shape of crystal domains. Distinct measures of structural information such as structure factors, two-particle correlation functions, order parameters (e.g., Q_{446} via 'shape spectroscopy') are not able to provide competitively detailed information [5–7], since the spatial resolution of our method is at an atomic level and neither restricted to mono-crystalline nor to ideal structures.

This paper addresses the problem of structure analysis using pattern recognition of the shape of the polyhedron formed by 'relevant' neighbors of any individual atom. The meaning of 'relevant' will be clarified below and is different from 'closest' and 'within first coordination shell'. The algorithm implements criteria for recognition of the two close packed crystal structures: hexagonal close-packed (hcp) and face-centered cubic (fcc), the almost

close packed body-centered cubic (bcc), and the icosahedral (ico) structure. The latter is expected to appear in case of amorphous solids or nanoclusters which tend to be close packed and as an intermediate phase during the transformation of structure, e.g., in the presence of external fields [8]. These four structures are considered for convenience and should be the most relevant for the study of dense fluids and metals modeled by radially symmetric potentials. The algorithm can also be adapted to recognize other structures such as simple cubic structure along the lines indicated in the following sections.

Concerning physical applications of this algorithm, the computer simulation of a homogeneous shear flow has shown the existence of shear induced changes even in a fluid-like colloidal dispersions subjected to high shear rates [9]. The colloids (or ‘atoms’) formed strings parallel to the stream lines which were sometimes ordered in a perfect hexagonal pattern when projected onto a plane orthogonal to the streaming direction. Similarly, for colloidal crystals it was also observed from snapshots and pair correlation functions, that they undergo a structural transition in which two-dimensional hcp (2D-hcp) layers are formed which are oriented to minimize the resistance against flow [10–16]. This ordering influences the rheological properties, e.g., enhance shear thinning, since the layered structure complies easily with the flow.

2. The program

Usually, as closest neighbors of an atom confined inside an ideal structure, atoms in its first coordination shell should be considered. In the following we give some arguments why to consider more than just the closest neighbors, the so called ‘relevant’ neighbors, in order to recognize the structure.

- (i) Taking into account physical reality, namely fluctuations, phonons and non-ideal lattices, it is relevant to note that for the body-centered structure the difference between radial coordinates of atoms within the first and second coordination shells may become very small. In fact, the diameter of the second coordination shell for ideal bcc is just 15.47% larger than the one for its first coordination shell. In contrary, for both, the ideal fcc and hcp structures, this difference is about 41.4%.
- (ii) Both the fcc and hcp lattice contain regular tetrahedra composed of four atoms. If we consider this lowest level, on which tendency of a material to be close packed can be satisfied, the similar conclusion can be made. The bcc crystal lattice is not composed of regular tetrahedra. The ratio of the edges in tetrahedra consisting only of atoms in the first coordination shell, $1 : 1 : 1 : 1.15 : 1.15 : 1.63$ (cf. Table 2) shows that the local tendency to form regular tetrahedra is not even partially fulfilled on the level of the first coordination shell. On the contrary, tetrahedra consisting of atoms from both first and second coordination shells resemble the regular tetrahedron ($1 : 1 : 1 : 1 : 1.15 : 1.15$).

For these reasons, we should include atoms of the second coordination shell for bcc structures into the analysis of structure. Due to thermal motion of particles atoms from the second shell easily become nearest neighbors in case of a bcc lattice, the first two shells in bcc structure are going to be mixed and they cannot be separated by the Voronoi analysis. This is demonstrated in Fig. 1, where already at low temperatures ($T = 0.0152$ in reduced units, see Section 3) the first and second maximum of the bcc structure are overlapping, qualitatively different from the case of fcc structure. The expected number of neighbors will therefore be 14 in the case of a bcc structure. The expected number of (the closest) neighbors for fcc and hcp structures is 12. The ico structure consists of atoms surrounded with 12 neighbors, which form 20 irregular tetrahedra. It is assumed that the first maximum in the pair correlation function of ico structure is at the same position as the first maximum of the other close-packed structures.

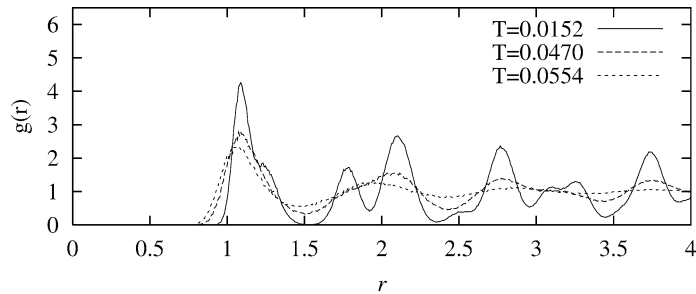
Let us call these particles ‘relevant neighbors’ of an atom.

The code RLSCODE makes use of the standard Voronoi construction [17] to determine relevant neighbors. The Voronoi method yields a polyhedron, defined as that region of space closer to the chosen atom than to any other.

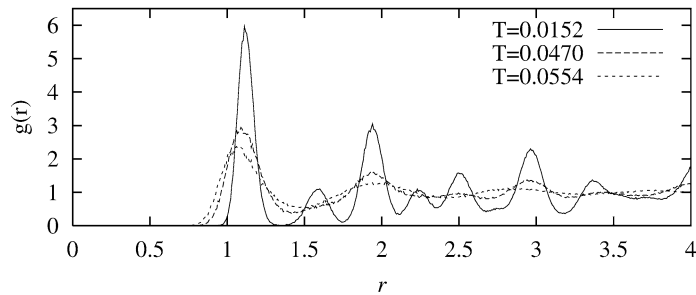
Table 2

Positions of the coordination shells I–IV, the cutoff radius—for clarity placed between shells II (bcc) and II (fcc/hcp)—and the number of the neighbors in coordination shell (in brackets), for three analyzed crystal structures

Type	I	II (bcc)	r_{cutoff}	II (fcc/hcp)	III	IV
fcc	1 (12)			$\sqrt{2} \approx 1.41$ (6)	$\sqrt{3} \approx 1.73$ (24)	2 (12)
hcp	1 (12)		~ 1.32	$\sqrt{2} \approx 1.41$ (6)	$2\sqrt{\frac{2}{3}} \approx 1.63$ (2)	$\sqrt{3} \approx 1.73$ (18)
bcc	1 (8)	$\sqrt{\frac{4}{3}} \approx 1.16$ (6)			$2\sqrt{\frac{2}{3}} \approx 1.63$ (12)	$\sqrt{\frac{11}{3}} \approx 1.91$ (24)



a) body-centered cubic structure



b) face-centered cubic structure

Fig. 1. The changes of pair correlation function with temperature for (a) bcc and (b) fcc structure at three temperatures $T/T_{\text{ref}} = 0.0152, 0.0470, 0.0554$.

Neighboring polyhedra, sharing at least a single point, define neighboring atoms. The minimum image convention and a cutoff, the distance beyond which atoms are assumed not to be neighbors are used. These measures can cause unreliable results for small and/or random systems, if the cutoff is chosen without care. To avoid that atoms from second coordination shell of fcc and hcp structures enter our analysis, and to ensure that atoms from the (overlapping) first and second coordination shells of bcc structures enter, a preselection is made by taking cutoff radius to be minimum of the global pair correlation function between the shell containing ‘relevant neighbors’ and the subsequent one, cf. Table 2. As shown below, for the purpose of our analysis of non-ideal lattices, this leads to stable results.

2.1. Criteria based on planar graphs

The first step of the analysis is therefore to extract the pair correlation function, the position of its first maximum, as well as the first relevant minimum, (procedure CUTOFFRAD, Table 3), and to extract from the list of potential neighbors a set of relevant neighbors by the Voronoi analysis (NEIGHBLST, Table 3). Next, by using the above mentioned cutoff a planar graph for each atom is established based on this set of relevant neighbors (STRUCTLST).

Table 3

Table of the main RLSCODE subroutines, their variables and actions. Few more subroutines existing in code are used internally and are not included here [22]

Name of subroutine	Arguments	Action, output
ORDER_START	–	opens <i>BCC.DM</i> , <i>FCC.DM</i> , <i>HEX.DM</i> , <i>ALL.DM</i> and <i>CRS.nb</i> files
ORDER_STOP	–	closing the <i>*.DM</i> and <i>CRS.nb</i> files
CUTOFFRAD	N,MX,MY,MZ,X,CL	function determines r_{cut} (RCUT)
NEIGHBLST	N,RCUT,MX,MY,MZ,X,CL, NNAB,NABLST	Voronoi analysis, which crates neighbor list. Output is stored in NNAB,NABLST variables
STRUCTLST	N,NABLST,NNAB,CELLTYPE	structures analysis CELLTYPE is output
STRUCTOUT	RTIME,N,X,CL,CELLTYPE NNAB,NABLST,PL	amounts of different structures and profile (axis: PL $\in \{1 : x, 2 : y, 3 : z\}$) are sent on standard output
DIRECTOUT	RTIME,N,X,CL,CELLTYPE NNAB,NABLST,NM	calculates angular distributions of neighbors and stores it to <i>*.DM</i>
CRSSCTOUT	RTIME,N,X,CL,CELLTYPE,NNAB, NABLST,RSTART,REND,PL	makes cross-section of the system and stores it to <i>CRS.nb</i>
PRESSURE	N,MX,MY,MZ,X,CL	function calculates pot. part of pressure

The neighbors are represented by nodes—the central atom is not included in the graph, and the nodes are connected with an edge if two neighbors of an atom are also neighbors of each other. The graph does only contain information about connections. Note, that atoms in set of neighbors of an atom do not have to be neighbors of each other.

The planar graphs are topologically different for each of the four structures of interest (cf. Fig. 2). A change of the orientation of a certain crystal structure does not result in topologically different planar graphs. The criteria to determine if the graph of a single atom is topologically equivalent with the planar graph of one of the structures is discussed next. The Euler theorem for planar graphs and further relations connecting the total number of the edges and the number of different surfaces—with three, four and more edges—into which the plane is divided by a planar graph, are used. The Euler theorem states that a connected and planar graph with n nodes and m edges divides the (infinite) plane into $f = m - n + 2$ surfaces. The theorem is derived by induction over the number of edges for any number of nodes [18]. We will illustrate the usefulness of the approach by giving an example on the bcc structure.

From the Euler theorem, the number of surfaces in case of bcc is 24 since the number of neighbors (nodes) is 14 and the number of edges is 36. Let us assume that there are surfaces also surrounded with more than three edges, e.g., with four edges. The number of these surfaces is denoted by Δ and \diamond for surfaces with three and four edges, respectively. The equations for surfaces and edges of the planar graph in this case read, respectively,

$$\begin{aligned} \diamond + \Delta &= 24, \\ 4\diamond + 3\Delta &= 2 \times 36. \end{aligned} \tag{1}$$

There is a single solution, $\Delta = 24$ and $\diamond = 0$. Similar relations can be written for the planar graph with same number of nodes and edges, which divides the plane into surfaces with arbitrary number of edges: Inserting $\sum_{x=3}^{\infty} \textcircled{x} = 24$ (with $\textcircled{3} \equiv \Delta$, $\textcircled{4} \equiv \diamond$ etc.) into $\sum_{x=3}^{\infty} x \textcircled{x} = 2 \times 36$ yields $\sum_{x=4}^{\infty} (x-3) \textcircled{x} = 0$. Since all \textcircled{x} 's are positive numbers, we have $\forall_{x \geq 4} \textcircled{x} = 0$. It is therefore proved that just the planar graph with 24 triangular surfaces does exist ($\textcircled{3} = 24$). Trying to combine 24 triangular surfaces in a planar graph, it is found that only one configuration is possible, the one characteristic for the bcc structure (Fig. 2). There are eight nodes with four edges and six nodes with six edges.

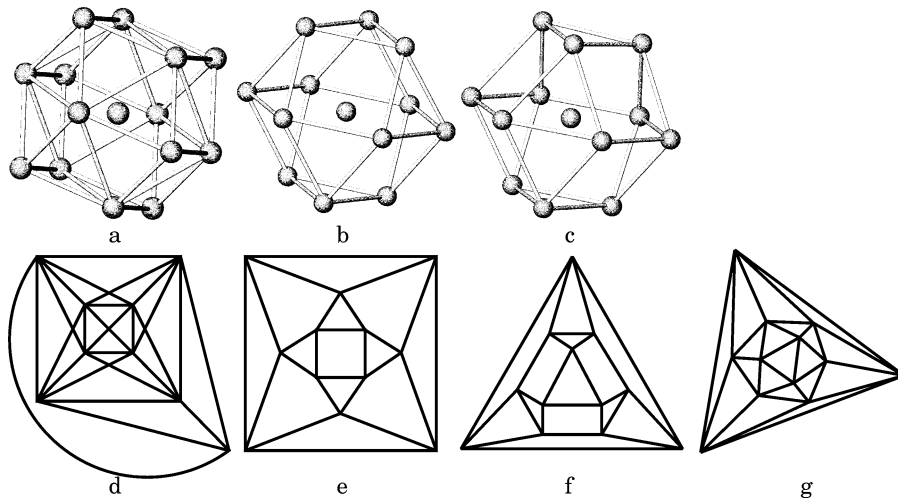


Fig. 2. The disposition of neighbors around atom in case of ideal crystal structures and the planar graphs defined on members of set of neighbors of one atom in bcc (a, d), fcc (b, e), hcp (c, f) and ico (g) structure. The nodes represent the neighbors and they are connected with a branch (edge) in case if they are also neighbors.

In bcc structure eight neighbors of the atom have four neighbors and the remaining six neighbors have six neighbors within the set of neighbors of the central atom. The minimum and sufficient criterion for bcc structure is: an atom is surrounded with bcc structure if it has 14 neighbors and eight of them have four neighbors and six of them six neighbors within the set of neighbors of the central atom.

In ico structure the atom should have 12 neighbors and each neighbor should have five neighbors (Fig. 2(g)). Both in the fcc and hcp structure the atom has 12 neighbors which form eight triangular and six square surfaces. While hcp structure has three pairs of triangular surfaces with the same edge, fcc structure has none and this fact is now used to distinguish between hcp and fcc, see Figs. 2(e)–2(f).

The ratio between all atoms which are found to belong to that structure (central atoms plus their neighbors, no double counting) and total number of atoms in the system is taken as a measure of the amount of certain crystal structure in the material.

2.2. Preparing the input data

The input data needed to evaluate the local structure consists of coordinates of particles, dimensions of simulation box and a free (time) parameter potentially used for animations, cf. Table 4.

2.3. Subroutines and general format of the output

The first step of the analysis is to determine the cut-off radius by using a subroutine CUTOFFRAD. Subroutine NEIGHBLST represents the standard Voronoi analysis. This routine takes in a configuration in a cuboid with periodic boundary conditions and for each atom obtains the information about relevant neighbors. Using cutoff radius subroutine NEIGHBLST eliminates atoms which are neighbors only in one point of space (relevant for perfect lattices). For bcc lattice the subroutine returns 6 closest atoms more than it would be expected from coordination number. The information about relevant neighbors is stored in NABLST—a two-dimensional matrix containing the list of indices of relevant neighbors and an array NNAB which contains the number of relevant neighbors for each atom.

The subroutine STRUCTLST performs the analysis of neighbor displacements and returns a matrix with $4N$ elements: CELLTYPE. The information about structure that surrounds each of the atoms is stored in a four-

dimensional field of logical type. The field value is ‘true’ for an atom if it is found to belong to one of the following structures 1 : fcc, 2 : hcp, 3 : bcc and 4 : ico. For any atom only one of these field values can carry the ‘true’ bit. If an atom belongs to none of the four structures all fields are ‘false’.

The information obtained by subroutines NEIGHBLST and STRUCTLST are treated and visualized by subroutines STRUCTOUT, DIRECTOUT and CRSSCTOUT. The relative amount of space occupied by fcc, hex, and bcc structure, as well as their combined amount and profiles are calculated by subroutine STRUCTOUT. Output of the latter procedure is directed to standard display. The subroutine DIRECTOUT calculates angular distribution functions of the relevant neighbors for the whole system and each of the crystal structures separately. The output is

Table 4
Summary of input and output variables used by subroutines

Parameter	Type	Limitations	Meaning
Input parameters			
N	integer	memory	total number of particles
X(#1,#2)	float	memory	coordinates #2 = (1 : x, 2 : y, 3 : z) for particle number #1 = 1, ..., N
CL(1-3)	float	> 0	cell dimensions (reduced units)
PL	integer	∈ {1, 2, 3}	axis normal to cross-section and axis of profile (1 : x, 2 : y, 3 : z)
NM	logical	.true./false.	.true. if neighbor angular distribution is to be normalized
RSTART	float	.. < CL(PL)/2	start of cross-section interval
REND	float	.. < CL(PL)/2	end of cross-section interval
RTIME	float	no	time parameter for animated output
Output variables			
RCUT	float	> 0	cut-off distance r_{cut}
MX,MY,MZ	float	> 3, < CL/RCUT	number of cells in x-, y-, z-direction, implemented value: CL/RCUT/2
NNAB(#1)	integer	memory	number of neighbors for particle #1
NABLST(#1,#2)	integer	memory	particle number of #2th neighbor of particle number #1
CELLTYPE(#1,#2)	logical	.true./false.	.true. if particle #2 has lattice type #1 ∈ {fcc(1), hcp(2), bcc(3), ico(4)}

Table 5

Summary of files being produced by RLSCODE run. Subroutine CREATEOUT creates angular distributions of directions to closest neighbors and stores them to files *ALL.DM*, *FCC.DM*, *HEX.DM*, and *BCC.DM*. File *CRS.nb* is created by procedure CRSSCTOUT. Indices are the time parameter, also used for creating animations, and the plane of the cross-section (1 : x, 2 : y, and 3 : z). The last column lists the appropriate Mathematica™ calls

File name	Format	Content	Call
<i>ALL.DM</i>	Mathematica™	neighbors of all atoms	ALLN[(time parameter value)]
<i>FCC.DM</i>	Mathematica™	neighbors of fcc atoms	FCCN[(time parameter value)]
<i>HEX.DM</i>	Mathematica™	neighbors of hcp atoms	HEXN[(time parameter value)]
<i>BCC.DM</i>	Mathematica™	neighbors of bcc atoms	BCCN[(time parameter value)]
<i>CRS.nb</i>	Mathematica™	cross-sections	CRSxxx[(time parameter value), (plane)] where xxx ∈ {FCC, BCC, HEX, ICO, NON}

saved to four files ALL.DM, FCC.DM, HEX.DM, BCC.DM, respectively for all atoms and atoms only surrounded with fcc, bcc and hcp structure. Cross-sections of the system in three orthogonal planes are visualized with the subroutine CRSSCTOUT. The output is stored in CRS.nb file. The output of the subroutines DIRECTOUT and CRSSCTOUT is in Mathematica™ format, see Table 5.

Subroutines are summarized in Table 3 and their parameters are collected in Table 4.

2.4. Installation procedure

In order to install RLSCODE unpack the folder RLSCODE .tar.gz within your working directory.

3. Test runs

In the following, we present two examples how to use the package RLSCODE to recognize structure of a model metal to be described in Section 3.1 subjected to (i) melting and (ii) shear at constant shear rate from MD and NEMD simulations under constant density and temperature.

3.1. Background on the model material

We should give in brief a background on the simulation method used to create the configurations to be analyzed in this section.

In order to study solid friction we adapted the embedded atom method in the spirit of Holian et al. [19]. The method was originated by Daw and Baskes [20] and resembles the fact that in metals the conduction electrons are not localized about the nuclei; the energy depends upon the local electron density, resulting in forces between ions that are many body in character, rather than simply pairwise additive. Accordingly one considers two contributions to the potential energy E of the whole system made up by N particles. There is a conventional binary interaction term through a two-body interaction potential Φ as function of the distance between interaction sites and a term stemming from an embedding functional $\mathcal{F}(\rho_i)$, which produces the effect of the electronic ‘glue’ between atoms. The quantity \mathcal{F} is a nonlinear function of the (local) embedding density ρ_i of atoms $i = 1, \dots, N$. It is constructed from the radial coordinates of surrounding particles and requires the choice of a weighting function $w(r)$.

A simple choice for the model functions Φ and \mathcal{F} leads to a generic model metal, called EMB according to Ref. [3]. For the binary potential function Φ we have

$$\Phi(r) = \phi_0 r_0^{-4} [3(h-r)^4 - 4(h-r_{\min})(h-r)^3], \quad r \leq h, \quad (2)$$

and $\Phi(r; r \geq h) = 0$, with an energy scale ϕ_0 , a length scale r_0 , and an interaction range h . The minimum of the potential (see Fig. 1(a)) is located at the distance $r = r_{\min} = 2^{1/6} r_0 \approx 1.12 r_0$ as for a Lennard–Jones potential and the well depth of the potential is: $-\Phi(r_{\min}) = \phi_0 r_0^{-4} (h - r_{\min})^4$. For reasons discussed in [19,21] we use the normalized Lucy’s weight function $w(r) = w_0(1 + 3r/h)(1 - r/h)^3$ for $r \leq h$, with $w_0 = w(0) = 105/(16\pi h^3)$. The particular simple parabolic embedding potential for EMB is

$$\mathcal{F}(\rho) = F_0 \phi_0 r_0^6 ((\rho - \rho_{\text{des}})^2 - (w_0 - \rho_{\text{des}})^2), \quad (3)$$

where ρ_{des} is the desired embedding number density and F_0 is the embedding strength, both being simulation parameters.

Throughout this section we investigate the ‘basic’ model metal for which the desired density $\rho_{\text{des}} = r_0^{-3}$ equals the particle number density $n \equiv N/V = r_0^{-3}$; $F_0 = 1$ and $h = 1.6 r_0$ are fixed.

3.2. Test run (i) MD computer simulation of melting

The first test run is concerned with the melting of the model metal EMB described in the previous section by means of a NVT molecular dynamic method for $N = 10,978$ particles, starting from an ideal fcc and bcc lattice, respectively. Basic details on the implementation of computer simulation method can be found in the literature [3,17]. Simulation with constant density $n/n_{\text{ref}} = 1$ have been performed. The temperature is increased stepwise by $\delta T/T_{\text{ref}} = 0.0006$ every 800th time unit in the range $T/T_{\text{ref}} = 0.005, \dots, 0.065$. Before temperature is increased configurations were saved to a file, which we provide here as test examples. The free simulation parameters for the model metal EMB can be chosen as follows: $T_{\text{ref}} = \phi_0/k_B = 40$ kK and $t_{\text{ref}} = r_0(m/e_{b,\text{ref}})^{1/2} = 1.3 \times 10^{-13}$ s, where $r_0 = 0.256$ nm, $e_{b,\text{ref}} = \phi_0 = 47.4 \times 10^{-18}$ J and $m = 1.790 \times 10^{-21}$ kg. The temperature is kept constant by rescaling the magnitude of the particle velocity which corresponds to the Gaussian constraint of constant kinetic energy. A cubic simulation box with volume V , and periodic boundary conditions are used. The axes x, y, z correspond to the initial crystal directions [100], [010], [001], respectively. The angles, in angular distribution plots, are introduced as the angle, ϕ , between projection of vector in xz -plane and z -axis taking the values in range $[-\pi, \pi]$ and the angle, θ , between y -axis and vector, its values are in range $[0, \pi]$. Cutoff radius is calculated only once for the configuration with the lowest temperature.

In Fig. 3, relative number of atoms found to be surrounded by neighbors, which resume (a) bcc and (b) fcc structure pattern, and relative volume occupied by atoms and their neighbors in these structures are presented. The evolution of potential part of pressure with increase of temperature is given for comparison. The relative volume is larger than relative number of atoms in fcc structure, since the crystalline parts of the sample are fragmented (Fig. 4). That results in fact that less than 4% atoms whose neighbors have fcc pattern, fill with their neighbors almost 30% of box volume. Occasional increases of observed crystalline structure after the increase of temperature can be explained as consequence of fluctuations.

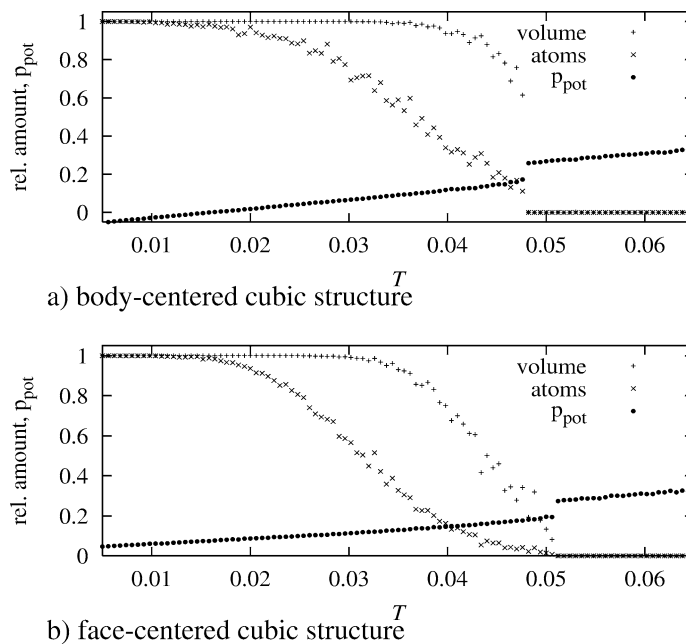


Fig. 3. Molecular dynamics simulation of melting, starting configuration is (a) bcc and (b) fcc. The relative number of atoms (\times) surrounded with crystalline structure, relative volume (+) occupied by atoms and their neighbors, and potential part of pressure (\bullet) are presented.

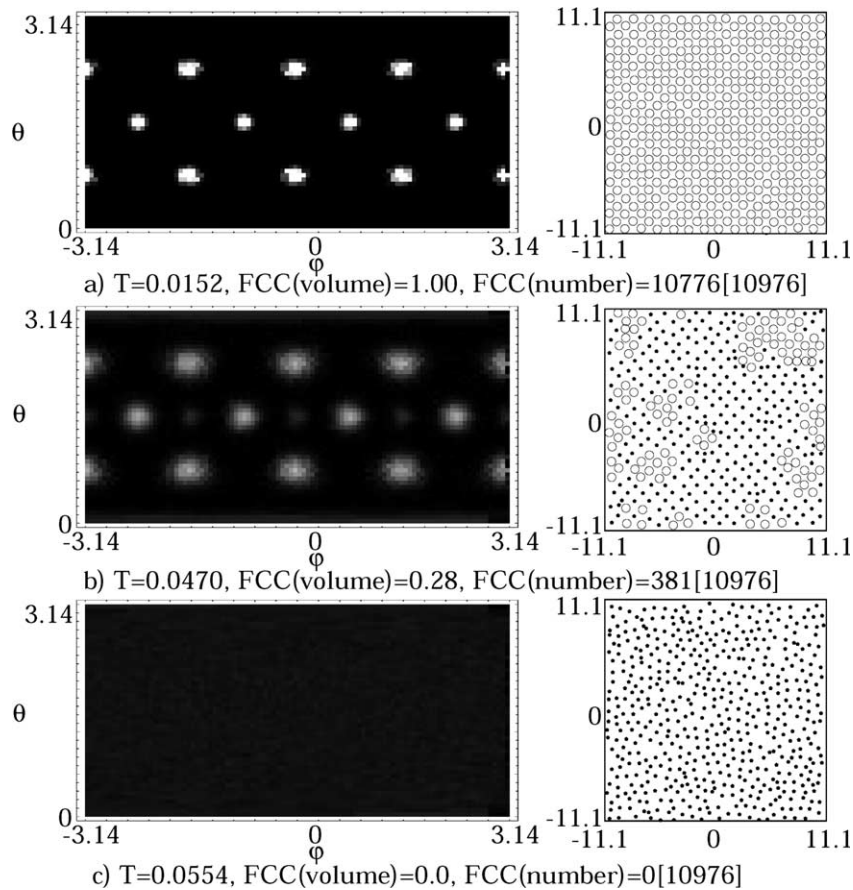


Fig. 4. The angular distribution of directions to the closest neighbors and cross-section of the system in plane $y = 0$ (the slice is $\delta y = 1$ wide). Dimensions of the system are $L_x, L_y, L_z = 22.2$. The plane of cross-section corresponds to [100] plane of the crystal. The atoms and their neighbors whose spatial distribution corresponds to fcc structure are represented with \circ , others are represented with \bullet . The evolution of the system with increase of the temperature is illustrated $T/T_{\text{ref}} = 0.0152, 0.0470, 0.0554$.

The changes in the fcc lattice with the temperature are illustrated in Fig. 4 with the cross-section in plane $y = 0$ (the crystal plane [100]) and angular distribution of directions to the closest neighbors of atoms for three different temperatures $T/T_{\text{ref}} = 0.0152, 0.0470, 0.0554$, the number of atoms and relative volume are given for comparison. The slice is $\delta y = 1$ wide.

At temperature $T/T_{\text{ref}} = 0.0470$, a greater dispersion of atoms around these maximums is visible. At melted state, the angular distribution of neighbors is uniform, and on cross-section of the system absence of the any order is visible.

The mixing of atoms of first and second coordination shells can be observed—as the points between angular distribution function maximums of original structure at temperature $T/T_{\text{ref}} = 0.0470$. This can be also observed in the pair correlation function of the same system given in Fig. 1.

3.3. Test run (ii) NEMD computer simulation of steady shear-flow

For the case of a model metal under steady shear-flow, a relative motion in the x -direction is simulated, with a load and shear gradient in y -direction. Simulation with constant temperature $T/T_{\text{ref}} = 0.008$ and constant density

$n/n_{\text{ref}} = 1$ is performed for $N = 17,576$ particles, where the initial positions of the atoms are fcc lattice sites. The axes x, y, z correspond to the directions $[100], [010], [001]$ in the starting crystal structure, respectively, the shear plane corresponds to the (001) plane in the crystal. Shear rate is $\gamma = 0.01$ and a conventional (profile based) thermostat is used. We present a snapshot of the system after $\delta t/t_{\text{ref}} = 2000$ in Fig. 5. The initial configuration did not survive under the shear-flow. A new ordering of atoms took place and new fcc- and hcp-dominated structures appear (Fig. 5). A configuration, oriented to minimize the resistance to shear is visible, the direction of the shear is parallel to direction $[1\bar{1}0]$ in fcc structure—dominant peaks at positions $(\phi, \theta) = (\pm\pi/2, \pi/2)$ in Fig. 6. Six peaks at $\theta = \pi/2$ are the consequence of the existence of the two different orientations of fcc and hcp structures—a fcc or hcp mono-crystal has three peaks, separated by $\Delta\phi = 2\pi/3$. The existence of both types of hexagonal layer packing: fcc and hcp is a consequence of deviations of layer velocities from ideal profile and the fact that layers are not parallel with the shear plane (due to the influence of the boundary conditions). The traces of bcc structure are produced by transformation of a part of the dominating fcc structure; from Fig. 6 it is visible that these two structures are compatible. The output of the analysis looks like:

```

...
  AVERAGE COORDINATION NUMBER = 12.45756
  NUMBER OF ATOMS WITH 8 NEIGHBORS 1
  NUMBER OF ATOMS WITH 9 NEIGHBORS 8
  NUMBER OF ATOMS WITH 10 NEIGHBORS 85
  NUMBER OF ATOMS WITH 11 NEIGHBORS 852
  NUMBER OF ATOMS WITH 12 NEIGHBORS 9448
  NUMBER OF ATOMS WITH 13 NEIGHBORS 5274
  NUMBER OF ATOMS WITH 14 NEIGHBORS 1906
  NUMBER OF ATOMS WITH 15 NEIGHBORS 2
  NUMBER OF ATOMS WITH 16 NEIGHBORS 0
  NUMBER OF ATOMS WITH 17 NEIGHBORS 0
  NUMBER OF ATOMS WITH 18 NEIGHBORS 0
2-axis disc. DENS HEX DENS FCC DENS BCC DENS ICO DENS 1CRY DENS 2CRY [tLJ=2000.00]
  0.12431 0.54645 0.53005 0.31694 0.00000 0.95082 0.77596
  0.37294 0.33526 0.54335 0.36416 0.00000 0.90173 0.63584
  0.62157 0.35111 0.46222 0.35111 0.00000 0.89778 0.59556
  0.87020 0.58015 0.55725 0.06870 0.00000 0.87786 0.83969
  1.11883 0.53801 0.76023 0.16959 0.00000 0.94152 0.90643
  1.36746 0.43949 0.58599 0.26115 0.00000 0.91720 0.82803
  1.61609 0.41638 0.40956 0.11945 0.00000 0.78498 0.70307
...
  18.77150 0.32824 0.43130 0.36641 0.00000 0.89313 0.57252
  19.02012 0.20690 0.38424 0.58128 0.00000 0.93596 0.44335
  19.26875 0.17647 0.33333 0.56209 0.00000 0.92157 0.37255
  19.51738 0.28413 0.40221 0.44280 0.00000 0.92989 0.53506
  19.76601 0.30000 0.50455 0.30909 0.00000 0.86364 0.63636
  20.01464 0.14365 0.45304 0.50276 0.00000 0.93370 0.50276
  20.26327 0.28889 0.47222 0.52778 0.00000 0.91111 0.51111
  20.51190 0.45578 0.50000 0.27551 0.00000 0.88435 0.69048
show data about crystal structure...
  FCCnum = 2000.000000000 2998
  FCCvol = 2000.000000000 0.5454597473
  HEXnum = 2000.000000000 2695
  HEXvol = 2000.000000000 0.5134842992
  BCCnum = 2000.000000000 923
  BCCvol = 2000.000000000 0.1954938620
  ICONum = 2000.000000000 0
  ICOvol = 2000.000000000 0.0000000000
  crystal = 2000.000000000 0.8933204412

```

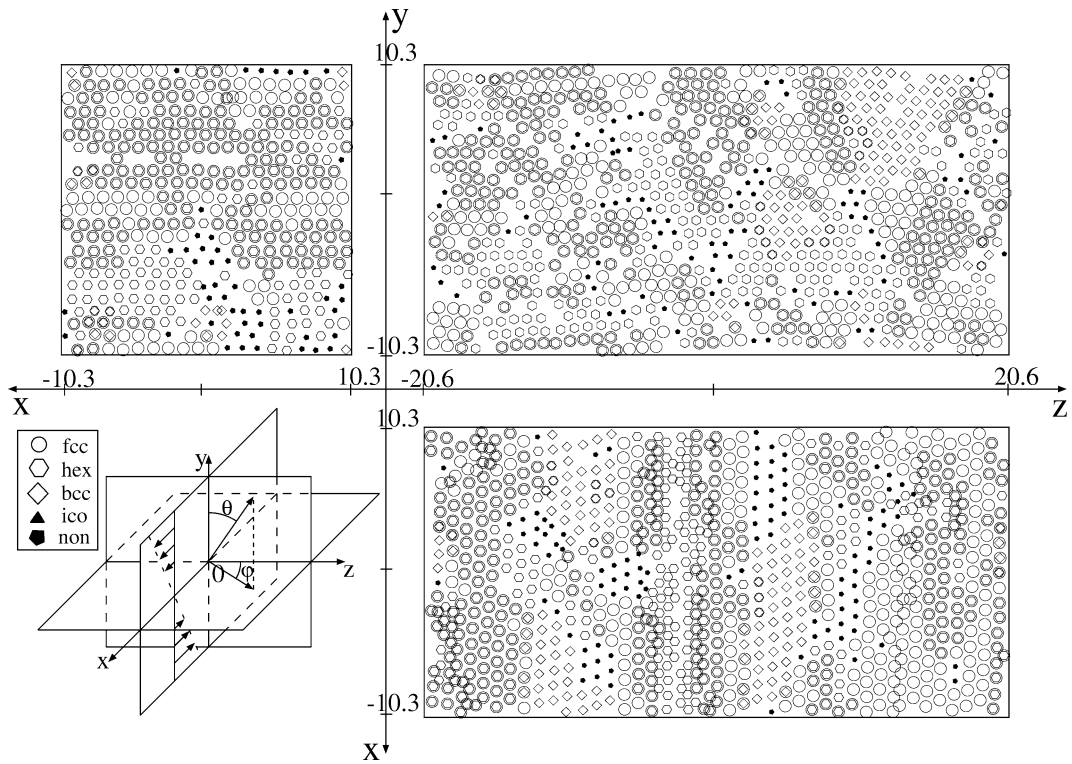


Fig. 5. NEMD snapshots of model metal indicating the type of local structure at $\delta t/t_{\text{ref}} = 2000$ after start of steady shear flow (with shear rate $\gamma = 0.01$ with shear is in x -direction and gradient is in y -direction). The start configuration is a fcc lattice, and x , y , z -correspond to the [100], [010] and [001] directions in the crystal, respectively. Cross-sections of the system are presented, in planes $x = 0$, $y = 0$ and $z = 0$, one length unit wide. Dimensions of the system are $L_x = 20.6$, $L_y = 20.6$, $L_z = 41.2$.

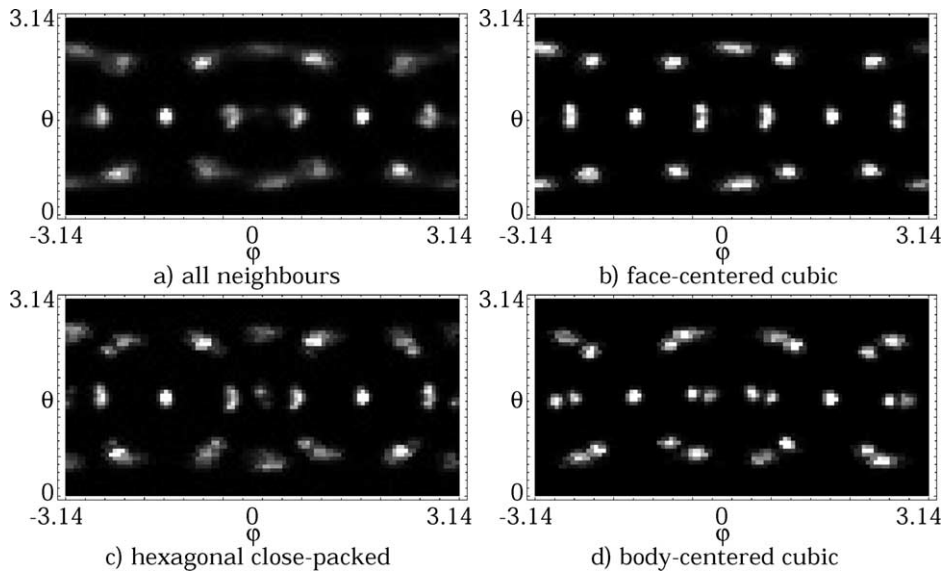


Fig. 6. The angular distribution of directions to the closest neighbors for all atoms in system and for every of three crystal structures detected bcc, fcc and hcp.

Table 6
Summary of error and warning messages and possible causes

Error message	Stop	Subroutine	Meaning/usual reason
change N	yes	main prog.	the number of particles is different from expected
increase MX,MY,MZ or MAXB	yes	CUTOFFRAD	the number of cells, system is divided in, is too small
decrease MX,MY,MZ	yes	NEIGHBLST	the number of cells, system is divided in, is too large
INCREASE IMPROFILE	yes	CUTOFFRAD	profile resolution too small
Warning message	Stop	Subroutine	Meaning/usual reason
LESS THAN 4 POINTS GIVEN TO WORK	no	STRUCTOUT	free volume, missing atom
TOO MANY VERTICES	no	NEIGHBLST	free volume, missing atom
LESS THAN 4 VERTICES FOUND IN WORK	no	WORK	free volume, missing atom
NONINTEGER NUMBER OF EDGES	no	WORK	free volume, missing atom
**** EULER ERROR: DEGENERACY ? ****	no	WORK	free volume, missing atom

3.4. Possible errors, runtime messages and extensions

Summary of error messages and possible causes are collected in Table 6. Messages resulting from the configuration of the system are not interrupting the execution of the program, as indicated in column ‘stop’.

Note added in proof

We lately became aware of the ‘common neighbor analysis’ (CN) structure recognition method [M.R. Sorensen, M. Brandbyge, and K. Jacobsen, Phys. Rev. B 57 (1998) 3283]. The CN uses rather a distance criterion with a fixed cutoff than a Voronoi construction with self-adjusting cutoff to recognize nearest (‘bonded’) neighbors. The CN method analyzes the neighbors in pairs and characterizes each pair with tree indices, while our method analyzes the displacement of all neighbors within the first coordination shell of an atom. The values of the three indices of the CN method can be also inferred directly from our planar graphs for those structures. The CN method cannot give information about orientation and planes of crystalline domains in polycrystalline configurations since it considers neighbors in pairs. CN method is more sensitive to first signs of crystal nucleation, which comes together with a higher sensitivity of the recognized structure to random processes.

Acknowledgement

Financial support by the Deutsche Forschungsgemeinschaft (DFG) via the Sonderforschungsbereich (Sfb) 605 ‘Elementarereignisse’ is gratefully acknowledged.

References

- [1] P. Entel, R. Meyer, K. Kadau, Philos. Mag. B 80 (2000) 183.
- [2] J.E. Hammerberg, B.L. Holian, J. Roder, A.R. Bishop, S.J. Zhou, Physica D 123 (1998) 330–340.

- [3] M. Kröger, S. Hess, *Z. Angew. Math. Mech.* 90 (Suppl. 1) (2000) 48–52.
- [4] M. Kröger, S. Hess, in: *Proc. XIII Int. Congress on Rheology*, Cambridge, Vol. 4, 2000, pp. 99–102.
- [5] B.J. Ackerson, W. Loose, *J. Chem. Phys.* 101 (1994) 7211.
- [6] A.Z. Patashinski, A.C. Mitus, M.A. Ratner, *Phys. Rep.* 288 (1997) 409.
- [7] A.C. Mitus, F. Smolej, H. Hahn, A.Z. Patashinski, *Europhys. Lett.* 32 (1995) 777.
- [8] J. Barker, M. Hoare, J. Finney, *Nature* 257 (1975) 120.
- [9] J.J. Erpenbeck, *Phys. Rev. Lett.* 52 (1984) 1333.
- [10] B.J. Ackerson, J.B. Hayter, N.A. Clark, L. Cotter, *J. Chem. Phys.* 84 (1986) 2344.
- [11] B.J. Ackerson, P.N. Pusey, *Phys. Rev. Lett.* 61 (1988) 1033.
- [12] B.J. Ackerson, *J. Rheol.* 34 (1990) 553.
- [13] R.L. Hoffman, *Trans. Soc. Rheol.* 16 (1972) 155; *J. Coll. Interf. Sci.* 46 (1974) 491.
- [14] H.M. Laun, R. Bung, S. Hess, W. Loose, O. Hess, K. Hahn, E. Hädicke, R. Hingmann, F. Schmidt, P. Lindner, *J. Rheol.* 36 (1992) 743.
- [15] S. Ashdown, I. Markovic, R.H. Ottewill, P. Lindner, R.C. Oberthür, A.R. Rennie, *Langmuir* 6 (1990) 303.
- [16] L.B. Chen, C.F. Zukoski, B.J. Ackerson, H.J.M. Hanley, G.C. Straty, J. Barker, G.J. Glinka, *Phys. Rev. Lett.* 69 (1992) 688.
- [17] M.P. Allen, D.J. Tildesley, *Computer Simulations of Liquids*, Oxford Science, UK, 1990.
- [18] L. Euler, in: H.-C. Im Hof (Ed.), *Series Prima. Opera Mathematica*, Birkhäuser, Basel, 1998.
- [19] B.L. Holian, A.F. Voter, N.J. Wagner, R.J. Ravelo, S.P. Chen, W.G. Hoover, C.G. Hoover, J.E. Hammerberg, T.D. Dontje, *Phys. Rev. A* 43 (1991) 2655.
- [20] M.S. Daw, M.I. Baskes, *Phys. Rev. Lett.* 50 (1983) 1285; *Phys. Rev. B* 29 (1984) 6443.
- [21] W.G. Hoover, S. Hess, *Physica A* 267 (1999) 98.
- [22] W. Press, S.A. Teukolsky, W.T. Vetterling, B.P. Flannery, *Numerical Recipes in Fortran*, 2nd edn., Cambridge Univ. Press, UK, 1992.